Supporting Information

Weakly-Dissociated Lithium Salt Decouples Solvent-Anion Interfacial Dynamics for Wide-Temperature Lithium-Ion Batteries

Shaoyun Zhou†, Zetai Xu†, Chaonan Wang†, Chao Tang, Junhua Jian, Meirong Wang, Hong-Bin Yao, Hongchang Jin, Yuhao Lu*, Hengxing Ji**

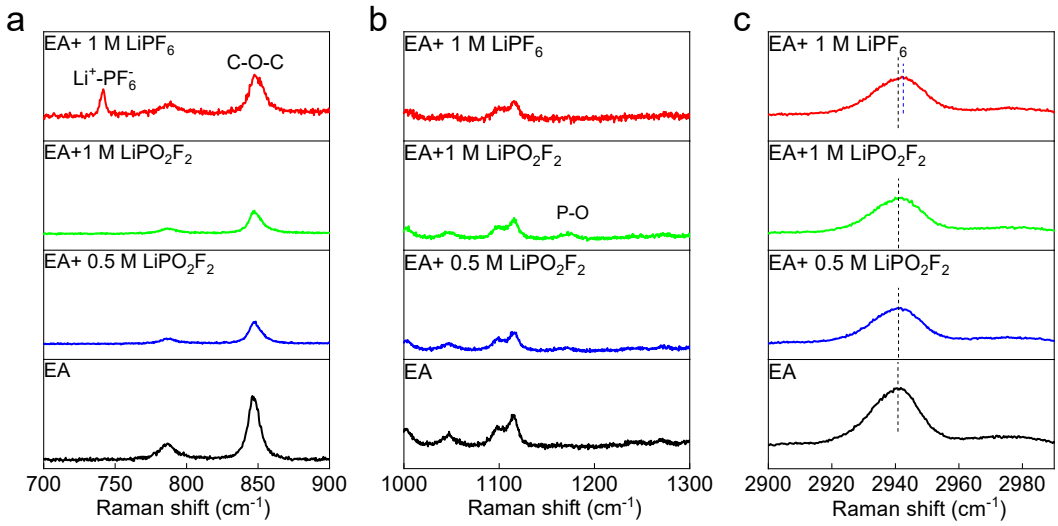

Figure S1. (a) Raman shifts from 700 to 900 cm^{-1} of EA and different solutions with $LiPF_6$ or LiDFP as salt respectively. (b) Raman shift from 1000 to 1300 cm^{-1}. (c) Raman shift from 2900 to 2990 cm^{-1}.

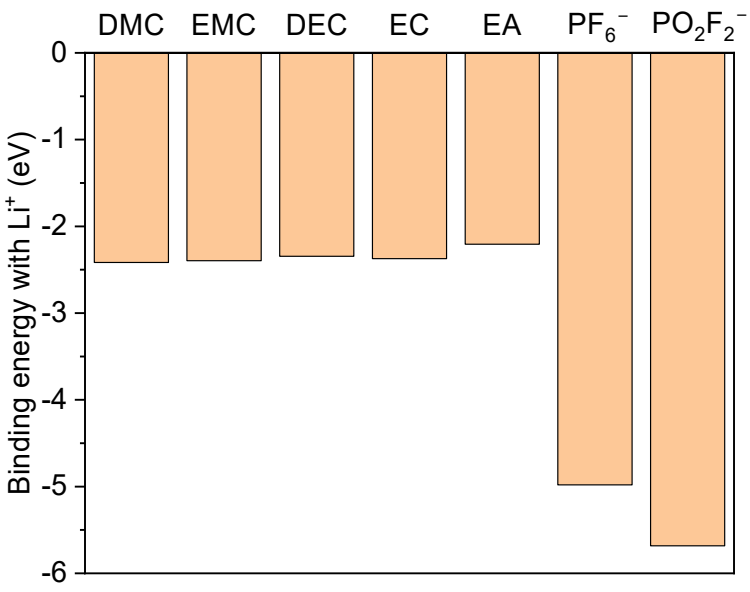

Figure S2. Binding energies of Li with different solvents, PF_6^- and $PO_2F_2^-$.

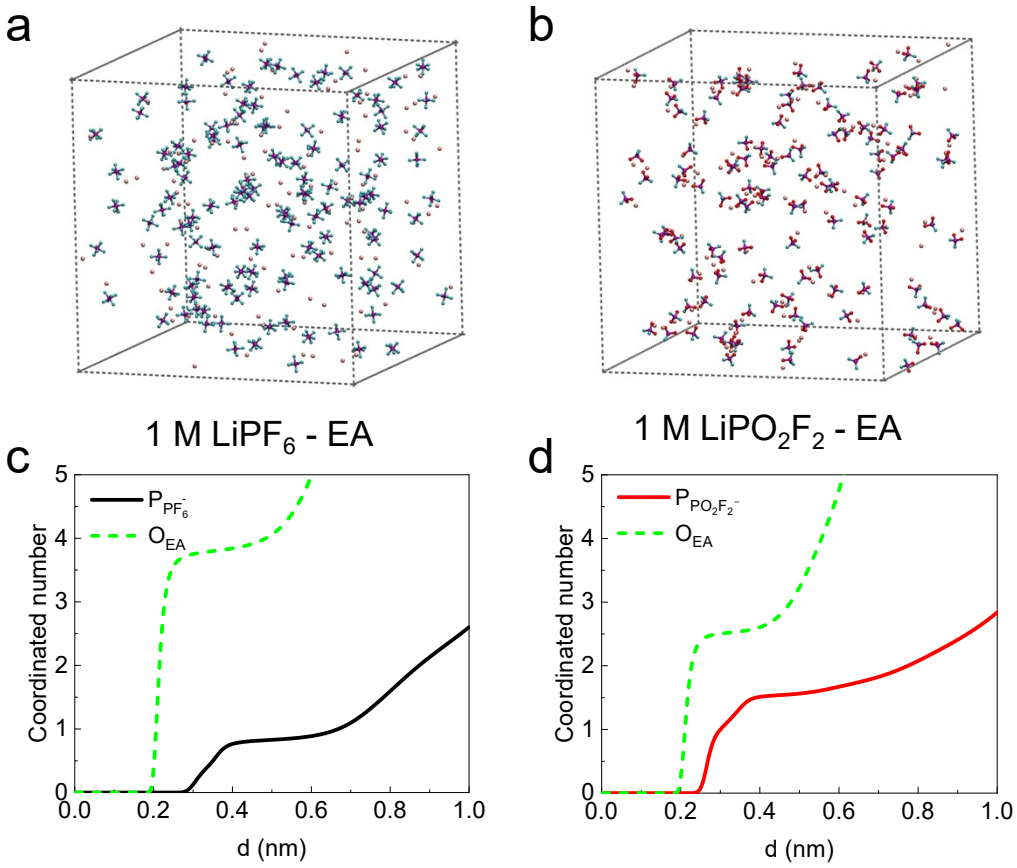

Figure S3. Snapshots of solvation structure obtained by MD simulation of 1 M $LiPF_6$ EA (a), 1 M LiDFP - EA (b). Li^+ coordination number in 1 M $LiPF_6$ EA (c), 1 M LiDFP EA (d).

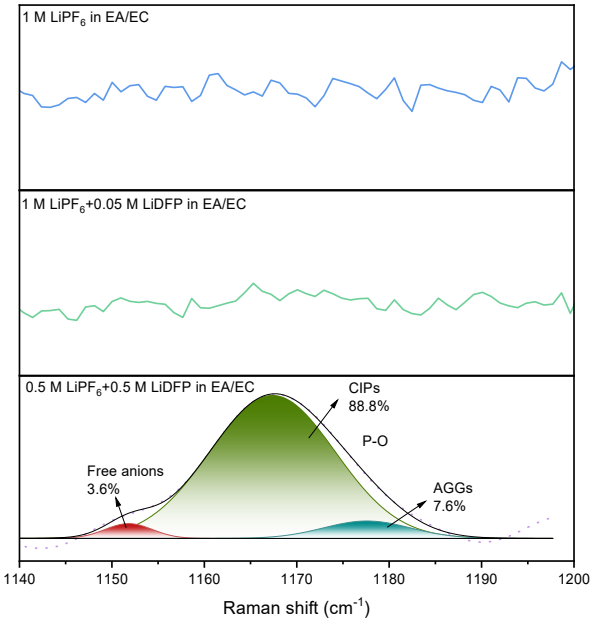

Figure S4. Raman shifts from 1140 to 1200 cm^{-1} of 1 M $LiPF_6$ EA/EC, 1 M $LiPF_6$ + 0.05 M LiDFP EA/EC, and 0.5 M $LiPF_6$ + 0.5 M LiDFP EA/EC electrolytes.

To experimentally validate the anion coordination predicted by MD simulations, we performed Raman spectroscopy and deconvolution analysis on electrolytes with varying LiDFP content (EA/EC co-colvent, 1 M $LiPF_6$ in EA/EC electrolyte, 1 M $LiPF_6$ + 0.05 M LiDFP in EA/EC electrolyte, and 0.5 M $LiPF_6$ + 0.5 M LiDFP in EA/EC electrolyte). In the P–O stretching region (1150–1180 cm^{-1}), a characteristic peak emerges and intensifies with increasing LiDFP concentration, indicating enhanced $PO_2F_2^-$ coordination. Following the referenced metho, we quantitatively distinguished free anions, contact ion pairs (CIPs), and aggregates (AGGs). As shown in Figure S4, free anions constitute only 3.6%, while CIPs and AGGs dominate at 88.8% and 7.6%, respectively. This distribution confirms that LiDFP exists predominantly as CIPs and AGGs, markedly increasing the $PO_2F_2^-$ coordination number in the primary Li^+ solvation shell, in excellent agreement with the MD simulations in Figure S3.

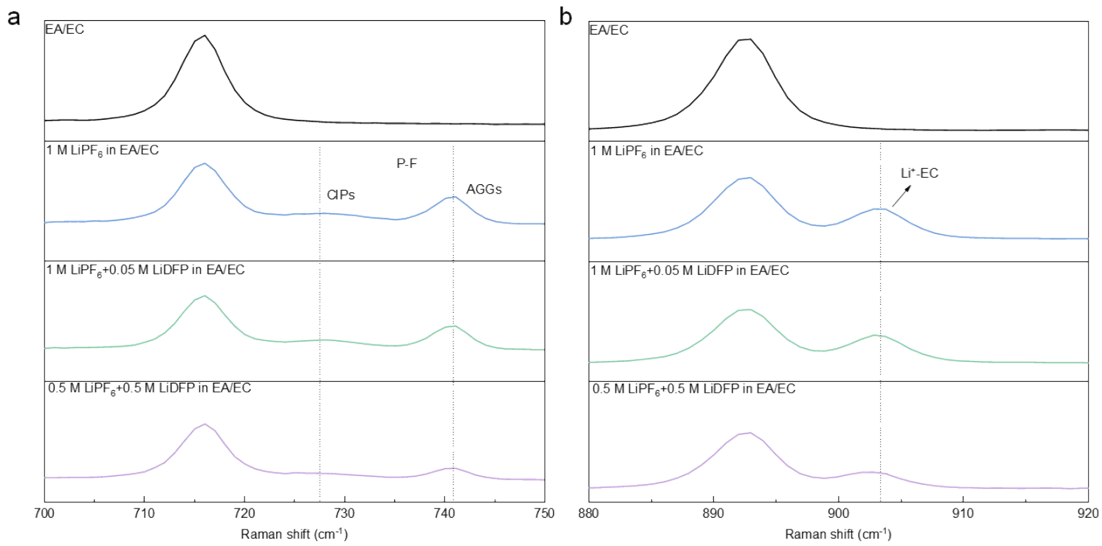

Figure S5. Raman shifts from (a) 700 to 750 cm^{-1} and 880 to 920 cm^{-1} of EA/EC, 1 M $LiPF_6$ EA/EC, 1 M $LiPF_6$ + 0.05 M LiDFP EA/EC, and 0.5 M $LiPF_6$ + 0.5 M LiDFP EA/EC electrolytes.

We further examined the P–F characteristic peak of $LiPF_6$ and the Li^+–EC coordination peak (Figure S5). Both peaks weaken significantly with higher LiDFP content, indicating reduced coordination of Li^+ with $LiPF_6^-$ and EC. These spectral trends are fully consistent with the MD results presented in Figure 2 of the manuscript, directly linking solvation structure to interfacial chemistry.

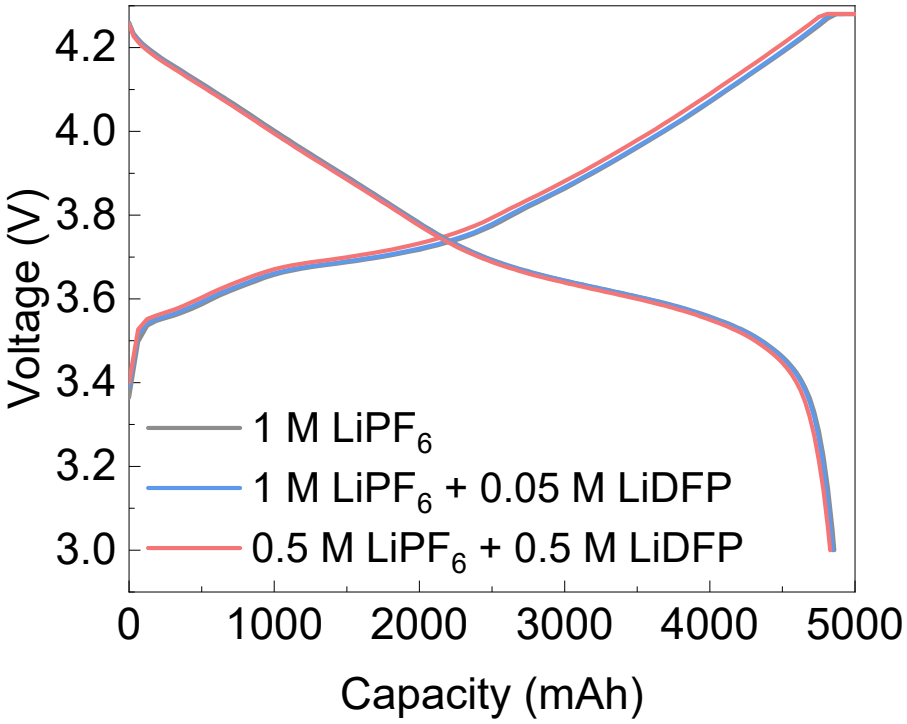

Figure S6. Charge–discharge curves of the NCM613||Gr pouch cells using various ratios of $LiPF_6$ and LiDFP mixed salts.

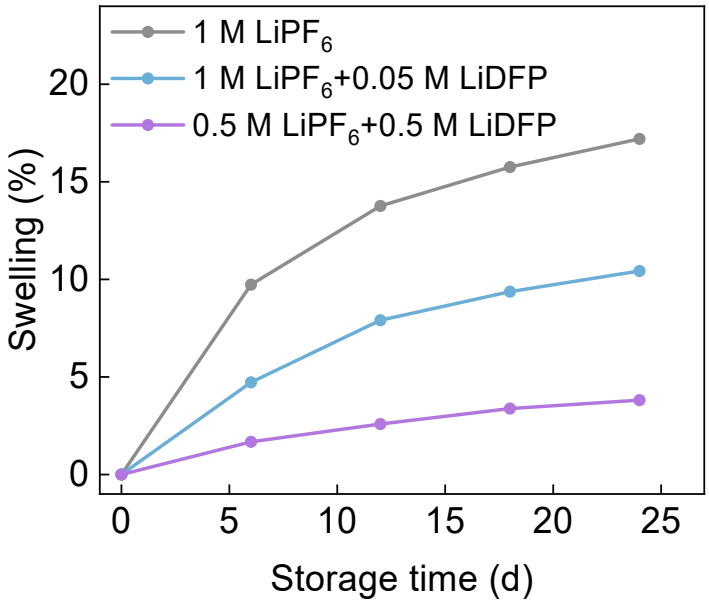

Figure S7. Swelling of the NCM613||Gr pouch cells stored at 60°C for 24 days using various ratios of $LiPF_6$ and LiDFP mixed salts.

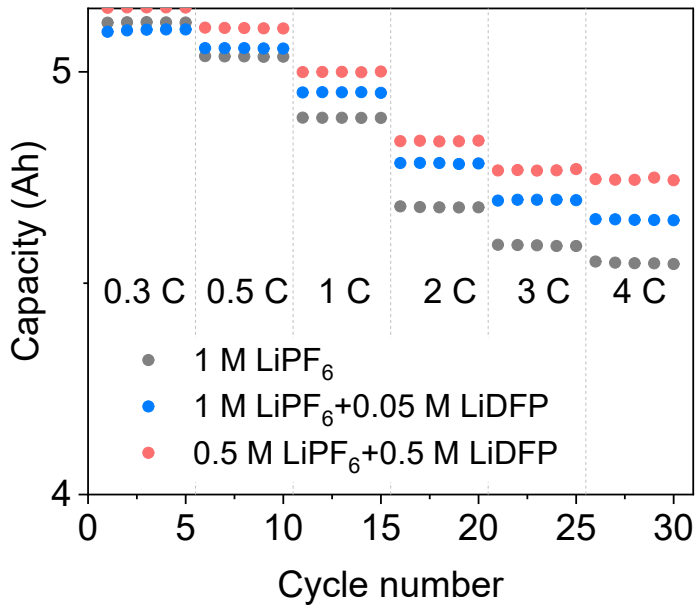

Figure S8. Rate performance of the pouch cells using various ratios of $LiPF_6$ and LiDFP mixed salts.

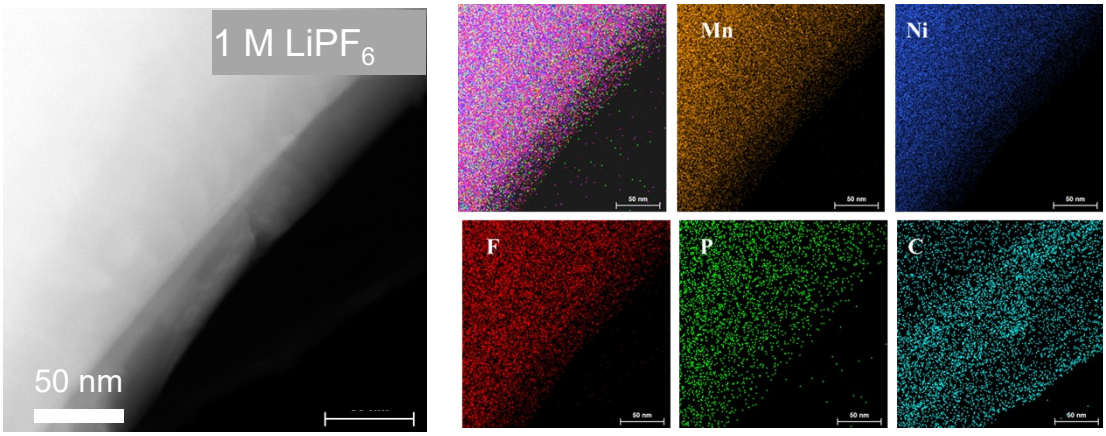

Figure S9. HRTEM HADDF images and elemental maps of the cathodes after the initial formation in 1 M $LiPF_6$ EA/EC electrolyte.

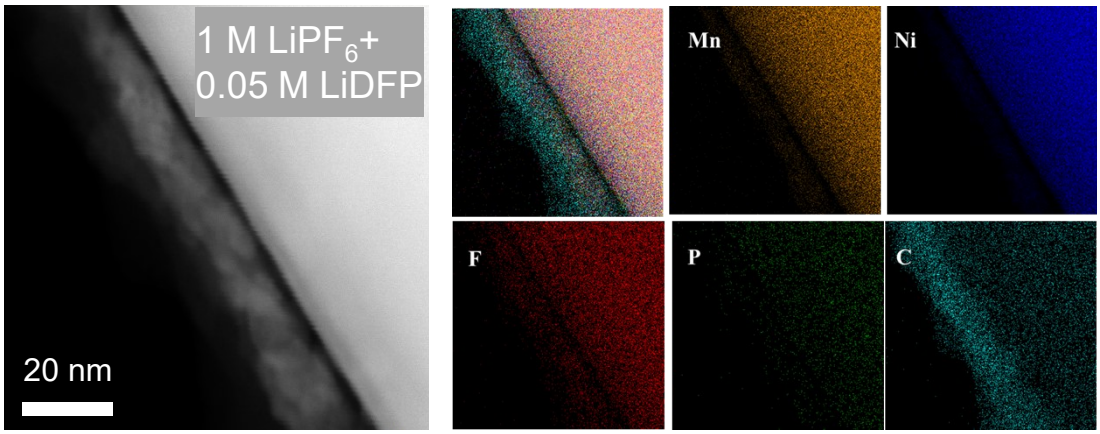

Figure S10. HRTEM HADDF images and elemental maps of the cathodes after the initial formation in 1 M $LiPF_6$ + 0.05 M LiDFP EA/EC electrolyte.

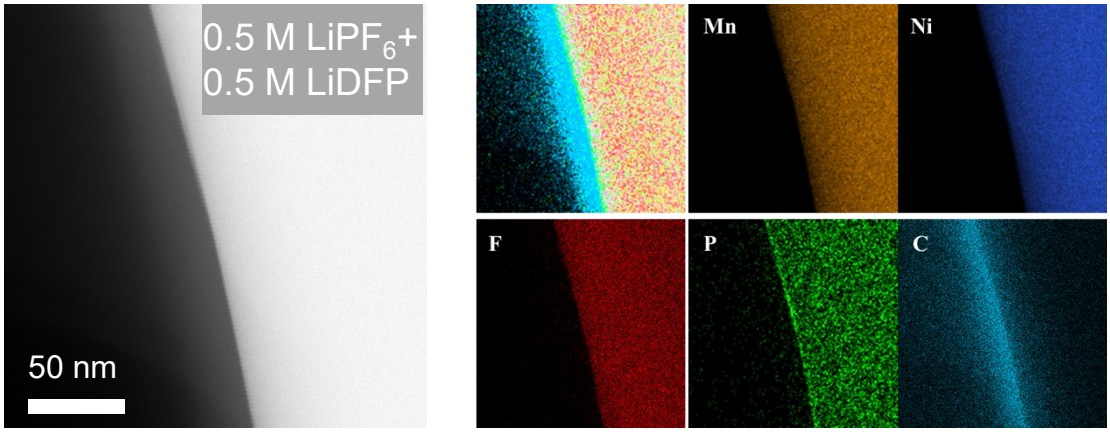

Figure S11. HRTEM HADDF images and elemental maps of the cathodes after the initial formation in 0.5 M $LiPF_6$ + 0. 5 M LiDFP EA/EC electrolyte.

Table S1. Several solvents' dielectric constants, DN, viscosity, and solubility of LiDFP

Solvent	Dielectric constant	DN	Viscosity / mPa·s	LiDFP solubility (25°C)/g
EA	6.0	17.1	0.45 (20°C)	>9
DMSO	46.4	29.8	1.99 (25°C)	>30
TEP	13.1	23.4	1.60 (25°C)	>20
DME	7.2	20.0	1.10 (20°C)	>29
SL	42.0	14.8	10.29 (30°C)	>25

Table S2. The conductivity of different LiDFP electrolytes.

Electrolyte formula	conductivity@25°C (mS/cm)
EA, 1.1 M LiDFP (Nearly saturated)	0.04
EA/EC=7/3, 1.5 M LiDFP (Nearly saturated)	0.62
EA/EC=7/3, 1 M $LiPF_6$	14.29
EA/EC=7/3, 1 M $LiPF_6$ + 0.05 M LiDFP	13.87
EA/EC=7/3, 1 M $LiPF_6$ + 0.5 M LiDFP	11.14
EA/EC=7/3, 0.5 M $LiPF_6$ + 0.5 M LiDFP	8.44

Table S3. Comparison of Li^+ coordination number in the first solvation sheath among three electrolytes.

Electrolyte	$P_{PF_6^-}$	$P_{PO_2F_2^-}$	O_{EC}	O_{EA}	$PO_2F_2^-/PF_6^-$	$PO_2F_2^-$ /Solvent
1 M $LiPF_6$	0.406	-	1.216	3.135	-	-
1 M $LiPF_6$ + 0.05 M LiDFP	0.399	0.077	1.190	3.047	0.193	0.018
0.5 M $LiPF_6$ + 0.5 M LiDFP	0.153	0.696	0.940	2.633	4.549	0.195

Table S4. Experimental context of the reported Gr-based full cell in Figure3f.

	Cathode	Anode	Voltage range	Cell format
Ref.45	NCM523	Gr	3.0-4.3V	Pouch cell
Ref.46	NCM811	Gr	2.8-4.3V	Pouch cell
Ref.47	$LiFePO_4$	Gr	2.5-4.2V	Coin cell
Ref.48	$LiCoO_2$	Gr	2.8-4.55V	Pouch cell
Our work	NCM613	Gr	2.8-4.28V	Pouch cell